Extracting information from axle-box acceleration: on the derivation of rail roughness spectra in the presence of wheel roughness

Tobias D Carrigan and James P Talbot

Department of Engineering, University of Cambridge, Cambridge, CB2 1PZ, UK
tdc41@cam.ac.uk, jpt1000@cam.ac.uk

Abstract. Railhead roughness increases over time, leading to increased environmental noise and vibration. The use of axle-box acceleration (ABA) measurements on in-service railway vehicles to monitor rail roughness is potentially more cost-effective than other techniques. The measured acceleration requires signal processing to derive suitable metrics of railhead condition. A transfer function may be calibrated with direct roughness and ABA measurements made on a reference track, which may then be used to derive roughness spectra from subsequent ABA measurements. However, this approach is affected by variations in track dynamic behaviour, as well as variations in wheel roughness, which is inherently combined with rail roughness in the ABA measurement. This paper proposes an improved approach that (i) extracts the track's dynamic stiffness parameters from the ABA measurements, enabling the derivation of the roughness-ABA transfer function for each section of track, and (ii) separates the wheel and rail roughness by synchronous averaging over several wheel revolutions. By accounting for variations in track properties and removing the influence of wheel roughness, initial modelling indicates that reliable measurements of rail roughness spectra can be obtained in practice.

Keywords: Axle-Box Acceleration, Rail Roughness, Corrugation, Wheel Roughness, Track Stiffness.

1 Introduction

The potential of axle-box accelerometers, mounted on in-service railway vehicles, has long been recognised as a cost-effective means of continuously monitoring the condition of railway track, without the need for dedicated measurement trains [1, 2]. An accelerometer measures the vertical motion of the axle-box as excited by irregularities on the running surfaces of the wheel and track. Axle-box acceleration (ABA) measurements have previously been analyzed through a variety of techniques, ranging from simple root-mean-square analyses [3] to time-frequency analyses [4], in order to detect corrugation and short track defects [5], for example. However, ABA alone cannot quantify rail roughness in absolute terms as it depends on vehicle speed and the dynamic properties of the vehicle and track, as well as wheel roughness.

This paper reports on progress towards deriving rail roughness spectra from ABA that are independent of vehicle speed, track dynamics and wheel roughness. The derivation requires knowledge of the transfer function from the roughness excitation to the axle-box response. This transfer function can be determined by comparing direct roughness and ABA measurements made on a reference track, as done for the High-Speed Rail Corrugation Analyzer (HSRCA) [6], Banverket's ABA system [7] and by Németh and Schleinzer [8], but the result is accurate only on track that is dynamically similar to the reference track at the time of calibration. In practice, the track's stiffness can vary significantly with location and time due to variations in track construction, soil properties and environmental conditions: trial HSRCA measurements [6] were affected by varying track properties at different locations, and ABA measurements on the UK West Midlands Metro have been found to vary seasonally with environmental conditions [9]. There is a clear need for improved methods.

2 Deriving roughness spectra from axle-box acceleration

By considering force equilibrium and compatibility of displacements at the wheel-rail interface, and assuming stationary random signals of rail roughness and ABA, the roughness power spectral density (PSD) $S_{\delta\delta}(\gamma)$ in the wavenumber (γ) domain may be derived from the frequency (ω)-domain PSD of ABA $S_{aa}(\omega)$ using random process theory [9, 10]:

$$S_{\delta\delta}\left(\gamma = \frac{\omega}{v}\right) = vS_{\delta\delta}(\omega) = \frac{v}{|H(\omega)|^2} S_{aa}(\omega) \tag{1}$$

where v is the vehicle speed and $H(\omega)$ is the transfer function from roughness excitation to ABA, which depends on the point receptances of the wheel $H_w(\omega)$ and rail $H_r(\omega)$, and the contact spring stiffness k_H:

$$H(\omega) = -\omega^2 \left(\frac{H_w(\omega)}{H_w(\omega)+H_r(\omega)+k_H^{-1}}\right) \tag{2}$$

An estimate of the rail roughness PSD may therefore be derived directly from the ABA PSD, given the vehicle speed and estimates of the wheel and rail receptances.

2.1 PSD calculation and roughness derivation procedure

Here, PSDs are calculated using Welch's method of averaging periodograms (square-magnitude discrete Fourier transforms) of overlapping segments of the signal. The length and number of segments are selected based on recommendations in EN 15610 [11] for plotting rail roughness spectra at wavelengths up to 1 m: 30 segments of length 4 m are used to attain the required accuracy [9]. The time-histories acquired over the respective segments are Hann-windowed and overlapped with each other by 50%, so the spectra are taken over 62 m of track.

The basic procedure for deriving the rail roughness PSD from an ABA signal recorded on a section of track is as follows. The track is split into 30 overlapping segments and the time-domain ABA signal is aligned with the segment boundaries ac-

cording to vehicle position and speed. Hann-windowed periodograms $S_{aa}(\omega)$ of the 30 ABA signal portions between segment boundaries are calculated and then converted into wavelength-domain roughness periodograms $S_{\delta\delta}(\lambda)$ using Equation (1), substituting $\lambda = 2\pi/\gamma$. These are then averaged together to give the final roughness PSD. Applying Equation (1) to the individual periodograms, rather than their average, reduces the effect of any variation in vehicle speed in the frequency-to-wavelength conversion [9]. This procedure can then be repeated on consecutive sections of track.

3 Simulator

A vehicle-track simulator has been developed to test the proposed algorithm. The simulator models an idealized vehicle-track system to calculate the ABA signal that would be measured as a wheel rolls along a given rail roughness profile. The ABA signal is fed into the roughness derivation algorithm under test, and the derived roughness spectrum is then compared to the actual roughness spectrum.

The simulator is based on the vehicle-track model illustrated in Fig. 1(a), which represents the track as an Euler beam on a continuous viscoelastic foundation that is discretized into finite elements [9] using the 'moving element' method developed by Koh *et al.* [12].

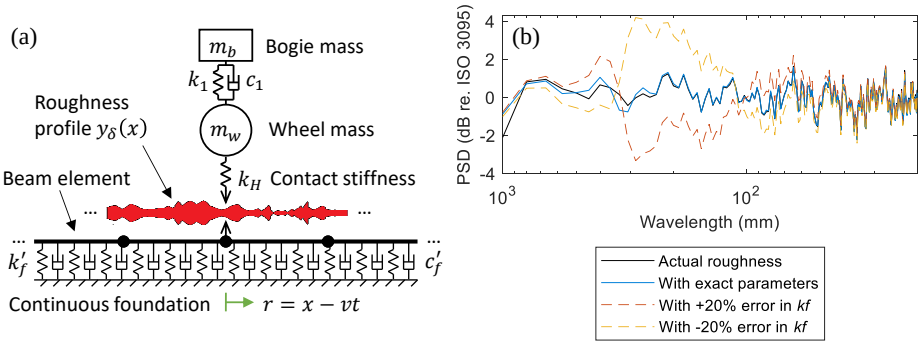

Fig. 1. (a) 2-DoF vehicle model on a moving-element beam on viscoelastic foundation with moving roughness profile. (b) PSDs of actual and derived roughness, relative to the ISO 3095:2013 limit spectrum, with exact model parameters and with ±20% error in track foundation stiffness k'_f.

3.1 Results for known vehicle-track parameters

The simulator is run along a random rail roughness profile with the vehicle and track parameters given in Table 1, which represent directly-fastened underground track [13]. The roughness profile is generated according to the roughness limit spectrum in ISO 3095:2013 [14]. Roughness PSDs are taken over 30 segments of length 4 m, overlapped by 50%, starting 5 m from the start of the simulation to avoid the initial transient in the model response. The roughness-to-ABA transfer function (Equation

(2)) is calculated using analytical point-receptance functions of the wheel and the rail, using the same vehicle and track parameters as the simulator (Table 1). The wheel receptance $H_w(\omega)$ corresponds to the mass-spring vehicle model of Fig. 1(a), and the rail receptance $H_r(\omega)$ is the frequency-domain solution for an Euler beam on viscoelastic foundation [9]. The actual roughness spectrum and three derived spectra (from the procedure outlined in Section 2.1) are plotted relative to the ISO 3095:2013 limit spectrum in Fig. 1(b); one of the derived spectra is obtained with the exact track parameters and two are obtained with ±20% error introduced into the track foundation stiffness k_f' used in the transfer function.

Table 1. Vehicle and track parameters used in the simulations [13].

Track parameter	Value	Vehicle parameter	Value
Wheel-rail contact stiffness k_H	1.35 GN m^{-1}	Vehicle speed V	20.0 m s^{-1}
Rail mass per length m_r'	56.0 kg m^{-1}	Wheel mass m_w	600 kg
Rail bending stiffness EI	4.86 MN m^2	Suspension stiffness k_1	1.40 MN m^{-1}
Foundation stiffness per length k_f'	77.0 MN m^{-2}	Suspension damping c_1	30.0 kN s m^{-1}
Foundation damping per length c_f'	32.8 kN s m^{-2}	Bogie mass m_b	1000 kg

If the exact parameters are known, the derived spectrum is very close to the actual spectrum. With the 20% deviation in the track stiffness, errors of up to 4 dB can be seen in Fig. 1(b) at wavelengths from 70 to 400 mm. This error is amplified because the P2 resonance frequency (near 62 Hz; wavelength of 0.32 m at 20 m/s) is shifted by the parameter deviation; this amplification increases with lower damping. This result indicates the importance of using an in-situ measurement of track stiffness where possible: errors can be reduced by ensuring that the natural frequencies of the transfer function match those of the actual vehicle-track dynamics.

4 Extracting foundation stiffness and damping

To improve the accuracy of the roughness derivation, it is clearly desirable to compensate for variations in track stiffness. At least three techniques are reported in the literature to extract track dynamic stiffness from vehicle acceleration measurements with the purpose of monitoring track for stiffness-related defects. Cano *et al*. [15] measured the frequency of the P2 resonance peak in the ABA spectrum and used a single mass-spring model to derive the associated track stiffness, knowing the combined mass of the unsprung vehicle components, rail and sleeper. Cano *et al*. report results within 16% of direct track stiffness measurements. Quirke *et al*. [16] and Zhu *et al*. [17] devised model-based optimization methods to identify track stiffness variations from bogie acceleration and ABA respectively. These methods fit the time-domain vehicle acceleration calculated by a vehicle-track model to measurements by setting the model's foundation stiffness parameters. The accuracy of the results presented by Zhu *et al*. [17] is initially near-perfect but is affected by measurement noise and the presence of a wheel flat. The stiffness identified by Quirke *et al*. [16] is within

6% of the actual stiffness in a simulated environment with 3% measurement noise but without rail roughness.

The method proposed here uses the present vehicle-track model (Fig. 1(a)) to identify the track's foundation stiffness and damping parameters from the P2 resonance, knowing all other model parameters. Here, a least-squares optimization is used to curve-fit the model's transfer function $H(\omega)$ (Equation (2)) to the square-root of the ABA PSD in the vicinity of the P2 resonance by optimizing the function's foundation stiffness and damping parameters, as well as its scaling. This method (along with the method of Cano *et al.* [15]) does not require the roughness to be known but assumes that it does not have features that alter the shape of the resonance peak in the ABA spectrum.

4.1 Results

The ABA spectrum resulting from the simulation in Section 3.1 is shown in Fig. 2(a). Here, spectra are calculated with an increased segment length of 8 m (covering 122 m of track) to improve the resolution of the resonance peak. The transfer function is assigned with the vehicle and rail beam parameters in Table 1 and is then curve-fitted to the ABA spectrum to identify the foundation stiffness k_f' and damping c_f'. The resulting values are given in Table 2, along with deviations from the actual simulated values. To examine the effect of errors in the wheel mass parameter m_w, the curve fitting is repeated with the wheel mass increased by 20%, and the resulting foundation parameters are given in Table 2 alongside the values with the actual wheel mass.

The result of deriving the roughness spectrum with the identified foundation parameters is plotted in Fig. 2(b), and is within 1 dB of the actual spectrum. The spectrum derived with the 20%-increased wheel mass is also plotted in Fig. 2(b), for both the actual and identified foundation parameters. The use of the identified, rather than actual, foundation parameters reduces the impact of the 20% error in wheel mass on the spectrum at longer wavelengths because the former corrects the transfer function's resonance frequency to match that of the vehicle-track system.

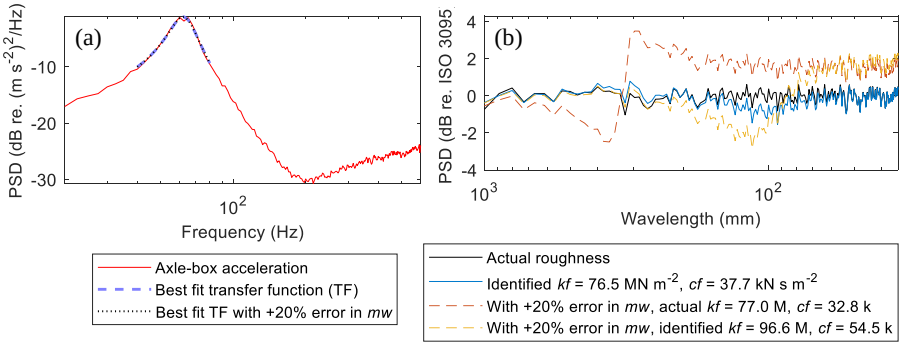

Fig. 2. PSDs of (a) axle-box acceleration and (b) actual and derived roughness relative to the ISO 3095:2013 limit spectrum, with identified track stiffness k_f and damping c_f parameters. Note that the three curves in plot (a) effectively overlap.

Table 2. Identified track foundation stiffness and damping compared to actual values.

Parameter	Actual value	Identified value for actual m_w	Identified value for 20%-increased m_w
Foundation stiffness per length k'_f (MN m^{-2})	77.0	76.5	96.6
Deviation in identified foundation stiffness		–0.7%	+25%
Foundation damping per length c'_f (kN s m^{-2})	32.8	37.7	54.5
Deviation in identified foundation damping		+15%	+66%

5 Separating wheel and rail roughness

The excitations associated with wheel and rail roughness are inherently combined in the response of the vehicle-track system. Unlike rail roughness, excitation by the wheel roughness is periodic with the rotation of the wheel. This makes it possible to separate the wheel- and rail-roughness components of an ABA signal by averaging together portions of the signal associated with each of a number of wheel revolutions, a process known as synchronous averaging [18].

The synchronous averaging technique was evaluated by Németh and Schleinzer [8] to extract the wheel component of ABA measurements before applying a transfer function to derive the wheel roughness spectrum, which agreed to within 1–5 dB of direct measurements depending on wavelength. Here, we evaluate this technique in a simulated environment with the aim of extracting rail roughness.

5.1 Method and results

To test the synchronous averaging technique, a wheel roughness profile is generated according to roughness measurements presented by Johansson [19] for powered wheelsets of the X2 locomotive. A rail roughness profile is generated according to the limit spectrum in ISO 3095:2013 [14] plus two sinusoidal corrugation components at wavelengths of 40 mm and 200 mm. The (actual) PSDs of wheel, rail and combined roughness are shown in Fig. 3. The simulator is run with the combined roughness profile at a vehicle speed of 20 m/s and with the model parameters in Table 1. The wheel component of the resulting ABA signal is extracted by averaging over 18 wheel revolutions (62.3 m of track as the wheel diameter is 1.1 m). The rail component is then derived by subtracting the wheel component from the combined ABA signal. The combined signal and both separated components are processed by Equation (1) and the procedure in Section 2.1 to derive the wheel, rail and combined roughness PSDs. All PSDs are computed using Welch's method over 62 m of track, split into 30 segments of length 4 m overlapped by 50%. This includes the wheel PSDs, which are facilitated by repeat-extending the wheel profile/component to cover 62 m of track. The derived wheel and rail roughness PSDs are also plotted in Fig. 3.

The derived rail roughness PSD (labelled "Derived rail (time domain sub.)") is close to the actual rail PSD at all wavelengths, including around the corrugation peaks

and where wheel roughness exceeds the rail roughness by up to 20 dB. The derived wheel PSD tends to be less accurate where it is less than the rail PSD, with errors of up to 5 dB.

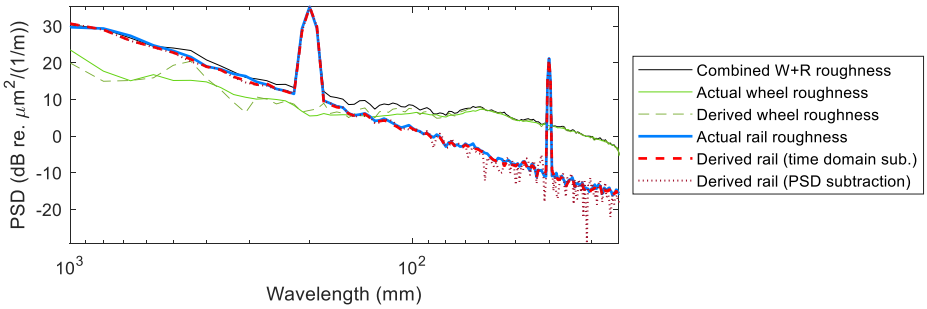

Fig. 3. Welch PSDs of derived wheel and rail roughness profiles compared to actual profiles.

An alternative rail roughness PSD is calculated by energy-subtracting the wheel roughness PSD from the combined PSD (labelled "Derived rail (PSD subtraction)" in Fig. 3). In contrast to subtracting in the time domain, the process of subtracting PSDs is affected by their statistical accuracy. The variance of the derived rail PSD increases as the wheel roughness PSD increases above the rail PSD. However, presenting the spectra in third-octave bands (not shown) averages out the variance, especially at shorter wavelengths where more PSD data points fall within a third-octave band, resulting in derived spectra that are within 1.5 dB of the actual ones. In most practical cases, wheel roughness does not exceed rail roughness at wavelengths longer than 300 mm, so energy subtraction may be sufficiently accurate for deriving the third-octave spectrum of rail roughness. This means that the wheel spectrum can be derived and updated on sections of track with conditions preferable for synchronous averaging (e.g. straight, invariant track) and then energy-subtracted from subsequent ABA-derived roughness spectra to obtain the rail roughness spectra.

6 Conclusions

By accounting for variations in track properties and removing the influence of wheel roughness, idealized vehicle-track modelling has indicated that reliable measurements of rail roughness spectra can be obtained from axle-box acceleration (ABA). Track dynamic stiffness parameters are extracted by curve-fitting a transfer function to the P2 resonance in the ABA spectrum. This method relies on sufficient spectral accuracy and resolution, and assumes that the roughness spectrum does not contain features near the P2 resonance that distort the ABA spectrum. Highly-damped resonances may also reduce accuracy. The synchronous averaging method of separating wheel and rail roughness assumes that the wheel excitation is perfectly periodic, which may not be true if the variation in lateral contact position on the wheel tread is considered.

Further work will develop the vehicle-track model and techniques, as necessary, to match the dynamics of real railway track. This will include considering discretely-

supported track and distributed mass and stiffness within the track slab/ballast, as well as variations in the lateral contact position. The techniques will be tested using real measurements of rail roughness and ABA, with the overall aim of developing an autonomous ABA-based measurement system that continuously 'maps' railhead roughness, enabling more efficient and proactive scheduling of rail maintenance.

References

1. Grassie, S.L.: Measurement of railhead longitudinal profiles. Wear 191, 245-251 (1996).
2. Talbot, J.P., Hunt, H.E.M., Hussein, M.F.M.: A prediction tool for the optimisation of maintenance activity to reduce disturbance due to ground-borne vibration from underground railways. Proc. 8th Int. Workshop on Railway Noise, Buxton, UK (2004).
3. Bocciolone, M. *et al.*: A measurement system for quick rail inspection and effective track maintenance strategy. Mech. Sys. Sig. Process. 21(3), 1242-1254 (2007).
4. Salvador, P. *et al.*: Axlebox accelerations: Their acquisition and time-frequency characterisation for railway track monitoring purposes. Measurement 82(C), 301-312 (2016).
5. Li, Z., Molodova, M., Núñez, A., Dollevoet, R.: Improvements in axle box acceleration measurements for the detection of light squats in railway infrastructure. IEEE Trans. Ind. Elec. 62(7), 4385-4397 (2015).
6. Bongini, E., Grassie, S.L., Saxon, M.J.: 'Noise mapping' of a railway network: validation and use of a system based on measurement of axlebox vibration. In: Maeda, T. *et al*. (eds.) Noise and Vibration Mitigation, NNFM 118, 505-513. Springer, Tokyo (2012).
7. Berggren, E.G., Li, M.X.D., Spännar, J.: A new approach to the analysis and presentation of vertical track geometry quality and rail roughness. Wear 265(9), 1488-1496 (2008).
8. Németh, I., Schleinzer, G.: Investigation into the indirect determination of wheel-rail surface roughness. Proc. Mini Conf. Vehicle System Dynamics, 135-146. Budapest (2008).
9. Carrigan, T.D., Fidler, P.R.A., Talbot, J.P.: On the derivation of rail roughness spectra from axle-box vibration: development of a new technique. Proc. Int. Conf. on Smart Infrastructure and Construction, Cambridge, UK (2019).
10. Newland, D.E.: An Introduction to Random Vibrations, Spectral and Wavelet Analysis. 3rd edn. Longman Scientific & Technical, Essex (1993).
11. EN 15610:2009: Railway applications – Noise emission – Rail roughness measurement related to rolling noise generation. CEN, Brussels (2009).
12. Koh, C.G., Ong, J.S.Y., Chua, D.K.H., Feng, J.: Moving element method for train-track dynamics. Int. J. Numerical Methods in Engineering 56(11), 1549-1567 (2003).
13. Grassie, S. L., Edwards, J. W.: Development of corrugation as a result of varying normal load. Wear 265, 1150-1155 (2008).
14. ISO 3095:2013: Acoustics – Railway applications – Measurement of noise emitted by railbound vehicles. International Standards Organisation (2013).
15. Cano, M.J., Fernández, P.M., Franco, R.I.: Measuring track vertical stiffness through dynamic monitoring. Proc. Inst. Civil Eng. – Transport 169(1), 3-11 (2015).
16. Quirke, P., Cantero, D., OBrien, E.J., Bowe, C.: Drive-by detection of railway track stiffness variation using in-service vehicles. Proc. Inst. Mech. Eng. F 231(4), 498-514 (2017).
17. Zhu, Q.X., Law, S.S., Huang, L.: Identification of Railway Ballasted Track Systems from Dynamic Responses of In-Service Trains. J. Aerosp. Eng. 31(5), 1-17 (2018).
18. Antoni, J.: Cyclostationarity by examples. Mech. Sys. Sig. Proces. 23(4), 987-1036 (2009).
19. Johansson, A.: Out-of-round railway wheels – assessment of wheel tread irregularities in train traffic. Journal of Sound and Vibration 293(3), 795-806 (2006).